

Partial pressure dependent in situ spectroscopic study on the preferential CO oxidation in hydrogen (PROX) over Pt/ceria catalysts

D. Teschner^{a,*}, A. Wootsch^b, O. Pozdnyakova-Tellinger^b, J. Kröhnert^a, E.M. Vass^a, M. Hävecker^a, S. Zafeiratos^a, P. Schnörch^a, P.C. Jentoft^a, A. Knop-Gericke^a, R. Schlögl^a

^a Fritz-Haber-Institut der Max-Planck-Gemeinschaft, Faradayweg 4-6, D-14195 Berlin, Germany

^b Institute of Isotopes, Hung. Acad. Sci., POB 77, H-1525 Budapest, Hungary

Received 18 January 2007; revised 10 May 2007; accepted 10 May 2007

Available online 19 June 2007

Abstract

Platinum supported on ceria can oxidize CO in excess hydrogen selectively (PROX process). In situ DRIFTS and high-pressure (~1 mbar) XPS experiments were performed to study the mechanism of the PROX reaction on Pt/ceria catalysts. The partial pressure of O₂ and/or CO was varied and correlated with induced changes in activity and selectivity as well as with the surface state and species under reaction conditions. Pt-carbonyl species changed rather insignificantly, especially relative to the wide variations of the product pattern with changing feed composition. Furthermore, the interconversion of formate and carbonate species was observed. Therefore, the changes in the evolution of surface species detected by in situ DRIFTS cannot explain the variation observed in CO oxidation activity. On the other hand, high-pressure XPS showed significant modification of the surface state with changing feed composition. Most significantly, oxygen vacancy formation seemed to correlate with enhanced CO oxidation activity. At higher vacancy density, water desorption was hindered. Highly hydrated ceria with significant vacancy density was found to be beneficial for the PROX process; here surface water blocked H_{ads} oxidation sites. Moreover, lower apparent activation energy of CO oxidation was measured in the PROX reaction on catalysts with more vacancies. The results given here reinforce the view of catalysts being adaptive to a certain reaction rather than having active sites as prepared. Whereas IR-detectable surface species may only be indicators and/or consequences of this surface change, formation of the beneficial surface/near-surface state may be the rate-limiting factor in several catalytic processes.

© 2007 Elsevier Inc. All rights reserved.

Keywords: Preferential CO oxidation; PROX; Platinum; Pt/CeO₂; Ceria; High-pressure XPS; In situ DRIFTS; Partial pressure dependence; Adaptive surface

1. Introduction

In fundamental catalytic research, two major routes are available to gain insight into catalytic function. Theoreticians use, for instance, density functional theory (DFT) calculations to acquire intrinsic kinetic data and apply them in kinetic Monte Carlo simulation for macroscopic modeling of elementary steps and comparison with experimental kinetic data [1–4]. This route is very effective in predicting reaction mechanisms, including adsorption energies and activation barriers of the elementary steps, albeit mainly on simplified surface units.

The other route involves the development and application of specially designed in situ spectroscopic experiments to collect information about the catalyst under working conditions and perform online product analysis [5–10]. Based on quantitative correlations of performance and spectral properties, the in situ methods provide experimental derivation of structure–function relationships and/or information on surface species present during catalytic turnover. Because none of the current in situ characterization techniques is capable of providing all of the information needed to gain a full understanding of catalytic function, combining the results of such in situ experiments is a highly desirable approach. In this study, we combine two complementary methods for studying Pt/ceria catalysts: in situ DRIFTS, which yields information mainly on the constitution of surface species, and high-pressure XPS, which reveals the surface elec-

* Corresponding author. Fax: +49 30 8413 4676.

E-mail address: teschner@fhi-berlin.mpg.de (D. Teschner).

tronic structure under reaction conditions. To take advantage of the full potential of the mentioned techniques (i.e., to differentiate between relevant and nonrelevant surface information), it is important to modify reaction parameters (i.e., temperature, partial pressure of reactants) and to relate the induced changes in reactivity to the in situ spectroscopic observations.

The preferential oxidation of CO (PROX reaction) is one key process in the development of an economically feasible technology to produce hydrogen for proton-exchange membrane fuel cells (PEMFCs) [11,12]. The concentration of CO in the upstream of hydrogen production unit (by, e.g., a steam-reforming process) must be kept as low as possible (preferentially in the low ppm region) by using sequential water–gas shift (WGS) and PROX units [13]. Pt/ceria catalysts can be used in both processes [14–18].

Recently, we reported on the in situ spectroscopic characterization of ceria-supported Pt [18] and Pd [19] catalysts during the PROX reaction. We assigned bands observed under reaction conditions by in situ DRIFTS and interpreted surface oxidation states revealed from in situ high-pressure XPS studies. The poor activity of Pd/CeO₂ in the PROX reaction can be clearly explained by the formation of detrimental Pd-hydride [19]. However, these studies were limited to one given concentration of reactants (i.e., 1% CO and 1% O₂ in H₂), which cannot provide sufficient information about the reaction mechanism. In the present study, Pt/CeO₂ catalysts were examined using the aforementioned in situ techniques under variation of the partial pressure of O₂ and/or CO in the reactant feed, and the catalytic pattern was correlated with the surface information. Although our catalysts prepared by the simple impregnation technique are likely not the best PROX catalysts, they still are able to remove 99% of CO from a model feed and thus are suitable for use in mechanistic studies. The in situ experiments were somewhat limited to slightly higher temperature than the optimal condition of best CO removal (due to charging effects in XPS and possible water condensation in the DRIFTS cell), but the systematic variation of reaction parameters during the spectroscopic experiments clearly allowed us to derive essential correlations between surface state/species and activity.

2. Experimental

2.1. Catalysts

This study used two catalysts with nominal metal loadings of 1 and 5% [18] prepared by wet impregnation with an aqueous solution of Pt(NH₃)₄(OH)₂. The impregnated samples were dried at 393 K overnight, calcined for 4 h at 773 K in flowing air, and reduced at 673 K for 4 h in flowing H₂. Dispersions determined by low-temperature H₂ adsorption [20] were $D = 62\%$ for 1% Pt/CeO₂ and 18% for 5% Pt/CeO₂.

We have previously reported that similar catalytic results as well as infrared spectra were observed on both 1 and 5% Pt/CeO₂ samples [18]. For the sake of clarity, here we present only the results of the 1% sample except for the high-pressure XPS experiments, in which the 5% Pt/CeO₂ [21]

produced less charging and Pt 4f spectra with satisfactory quality.

2.2. Catalysis

Catalytic tests were carried out at 383 K in an atmospheric continuous-flow glass reactor system as described previously [18]. Before catalytic testing, a charge of 43 mg of 1% Pt/CeO₂ was activated in situ in flowing air at 573 K, and between different measurement series, it was reactivated by the same air treatment at 573 K. The flow of reactant feed was 100 N mL/min (GHSV = $\sim 190,000\text{ h}^{-1}$), containing 0.5–4% CO, 0.2–4% O₂ (oxygen excess, λ , from 0.8 to 2) and the balance H₂. Oxygen excess is defined by the ratio of 2-times $p(\text{O}_2)/p(\text{CO})$ in the inlet stream (where $\lambda = 1$ corresponds to a stoichiometric mixture). The amount of catalyst used here did not allow achievement of the maximum conversion but was well suited to clarify the effect of the feed composition. In a separate experiment, apparent activation energies were determined in the range of 308–343 K (GHSV = $60,000\text{ h}^{-1}$) on a sample activated similarly in the same apparatus. Product analysis was performed using (i) a Balzers QMG 4211 mass spectrometer, (ii) a gas chromatograph with a thermal conductivity detector equipped with a polar column (Poropak Q) to separate CO₂ and H₂O from the other effluent gases, or (iii) a hydrogen-compensated flue-gas analyzer (MRU DELTA 65-3) for CO and O₂ quantification.

2.3. In situ DRIFTS

A diffuse reflection attachment (Selector, from Graseby Specac) was placed in a Bruker FTIR spectrometer equipped with a D315M MCT detector to collect DRIFT spectra. Reactions were conducted in a gold cup (2.5 mm high, 8.5 mm o.d., 7.2 mm i.d.) placed in a Graseby Specac environmental chamber with a ZnSe window. A spectrum of KBr recorded in N₂ served as background. Inlet gases were analytical grade and controlled by mass flow controllers. The total gas inlet was 50 N mL/min, containing 0.25–4% CO and 0.25–2% O₂ in H₂.

The measurements were carried out on a ca. 150 mg 1% Pt/CeO₂ sample previously pretreated in situ in flowing air at 573 K. The catalyst was purged in N₂ while cooling to 383 K, and then the reaction mixture (premixed in a bypass) was introduced to the catalyst in a single step. Spectra were collected as a function of contact time for at least 30 min in all cases, ensuring that steady-state operation was reached. Only spectra obtained under the steady-state conditions are shown. Gas composition was analyzed by a Pfeiffer OmniStar mass spectrometer.

The following IR bands were used for quantification of the surface species of interest [18]: formates, 3000–2675 cm⁻¹; carbonyls, 2100–1880 cm⁻¹; carbonates, 1150–970 cm⁻¹; water (including individual OH groups), 3750–2600 cm⁻¹ (here formates subtracted). The original spectra were transformed into the Kubelka–Munk function. Baselines were subtracted according to the profile of the spectral background, and bands were integrated.

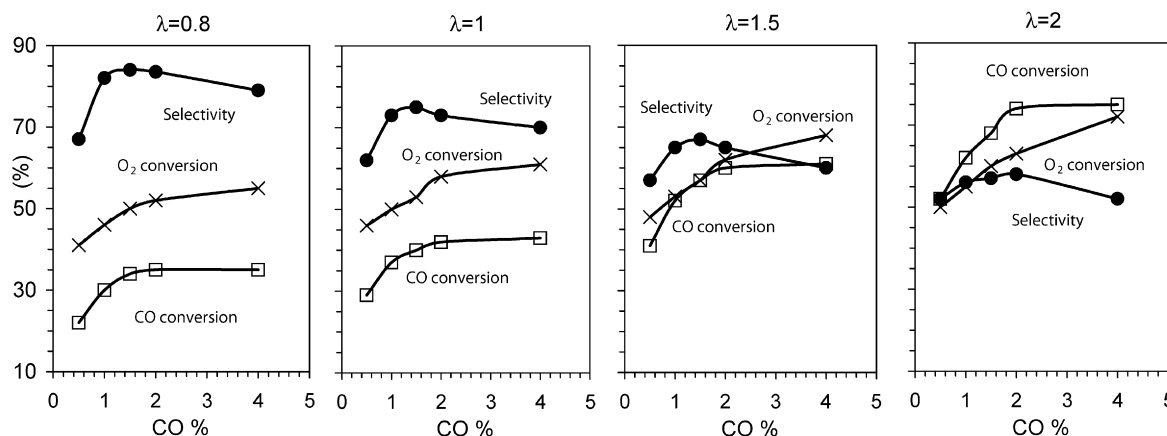


Fig. 1. CO oxidation activity and oxygen conversion in different PROX feeds on 43 mg 1% Pt/CeO₂ catalyst (GHSV = 190,000 h⁻¹) at 383 K as a function of CO content at different oxygen excess, λ . Hydrogen oxidation is the only side reaction decreasing PROX selectivity.

2.4. High-pressure XPS

The in situ XPS experiments were performed at beam line U49/2-PGM1 at BESSY, Berlin, Germany. Details about the setup construction as well as about the PROX experiments were published previously [18,22]. A pressed pellet of 5% Pt/CeO₂ containing about 100 mg of catalyst was activated in situ in oxygen (0.5 mbar, 573 K). The PROX mixture contained 0.72 mbar H₂, 0.03–0.24 mbar CO, and 0.015–0.12 mbar O₂, and the reaction temperature was set to 393 K. Gas flow (22–32 N mL/min) into the reaction cell was controlled using calibrated mass flow controllers and leak valves. Gas-phase analysis was performed with a quadrupole Balzers mass spectrometer connected to the experimental cell through a leak valve.

Ce 3d, O 1s, and Pt 4f spectra were recorded with photon energies of $h\nu = 1035, 660, \text{ and } 460 \text{ eV}$, respectively. The binding energies were calibrated using internal references, such as the Ce 3d v^0 (882.4 eV) and u''' (916.7 eV) states (where v^0 and u''' correspond to different final states) [23] or the Ce 4f state in the band gap.

3. Results

3.1. Catalytic reaction

Fig. 1 compares the CO oxidation activity and selectivity on 1% Pt/CeO₂ as a function of CO content and oxygen excess. CO conversion [$X(\text{CO})$] increased first and remained constant while the CO content of the feed was increased at constant oxygen excess (λ). Hence the amount of converted CO increased overproportionally at low CO content and scaled proportionally from 2% and above. On the other hand, oxygen conversion increased continuously with more CO and O₂ in the feed. Consequently, maximum selectivity was observed as a function of partial pressure, which was more pronounced at lower λ values. With higher oxygen excess, selectivity decreased and $X(\text{CO})$ clearly increased, whereas the increase in $X(\text{O}_2)$ was somewhat less pronounced. In addition (although not directly highlighted), higher $p(\text{CO})$ at constant oxygen partial pressure resulted in more CO₂ and less H₂O with approximately

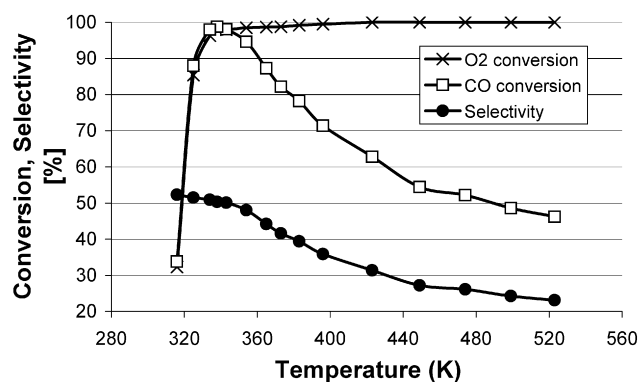


Fig. 2. Activity and selectivity of 1% Pt/CeO₂ in PROX feed of 1% CO, 1% O₂ ($\lambda = 2$) in H₂ (GHSV = 16,000 h⁻¹) as a function of temperature.

the same oxygen conversion. The higher CO oxidation rate at higher $p(\text{CO})$ is in contrast to the negative reaction order (-0.4) of CO observed on Pt/Al₂O₃ [24] but is in line with the data on gold catalysts, the CO reaction order being $+0.55$ on Au/Fe₂O₃ [25] and $+0.82$ on Au/TiO₂ [26].

In a separate experiment with a higher catalyst charge (GHSV = $\sim 16,000 \text{ h}^{-1}$), 1% Pt/CeO₂ was able to remove most of the CO—from a feed containing 1% CO and 1% O₂ in H₂ at lower temperature. The best CO removal was achieved at 333–343 K, with 98–99% conversion (Fig. 2).

3.2. In situ DRIFTS

Different formates, carbonates, and carbonyls were identified on ceria-supported Pt catalysts by IR spectroscopy during the PROX reaction; details on band assignment can be found in [18]. Fig. 3 compares the steady-state DRIFT spectra of Pt/CeO₂ recorded during PROX reaction at low (0.25% CO and 0.25% O₂) and high (4.1% CO and 2% O₂) feed CO concentration. In the region of OCO vibrations, intense bands of different types of carbonates were present. The $\nu(\text{CO}_3)$ bands of unidentate (1464, 1358, and 1085 cm⁻¹) and bidentate carbonate (1565, 1298, and 1010 cm⁻¹), as well as some polymeric carbonate species (1470, 1353, and 1045 cm⁻¹), were observed [27,28]. OCO vibrations of formate species, which

were also identified from the corresponding CH vibrations (2717 , 2837 – 2845 , 2935 , and 2950 cm^{-1}), were also visible at 1800 – 1000 cm^{-1} [29,30]. Intense broad, however poorly resolved $\nu(\text{OH})$ bands of hydroxyl groups indicated hydrogen bonded adsorbed water on Pt/CeO₂, as reported earlier [18]. A pronounced band representing linearly adsorbed carbonyls appeared at around 2050 cm^{-1} . Interestingly, a carbonyl band with almost the same intensity was observed at both low and high CO concentrations. The reaction product, CO₂, can be quantified from both IR and MS data. The catalytic MS data observed during the in situ DRIFTS experiments are compared in Table 1. Although the temperature in these experiments ($T = 383$ K) was beyond the optimal temperature for Pt/CeO₂ [17], we decided to work above 373 K to decrease the possibility of water condensation and enhance the effect on selectivity. Further, activity trends observed in the DRIFTS cell were similar to those in flow reactor but with different nominal values. Two sets of experiments were performed:

- (i) At low CO concentration, the oxygen excess was increased until CO oxidation was enhanced only insignificantly.
- (ii) CO was added stepwise to the previous mixture (with high oxygen excess).

Generally, oxygen conversion was very high and remained nearly constant during these experiments. When the concentration of inlet oxygen was increased, CO₂ production—and $X(\text{CO})$ —increased asymptotically but still remained quite low, whereas $X(\text{O}_2)$ slightly and selectivity strongly dropped (Table 1). In contrast, adding CO to the oxygen-rich feed dramatically improved both CO₂ production and selectivity. CO conversion achieved a maximum, whereas $X(\text{O}_2)$ remained constant. All of these changes in the latter sequence indicate a strong positive dependence on the CO partial pressure. This can lead to the conclusion that the reaction is limited by the surface concentration of “adsorbed” CO; however, as we show later, this conclusion is not supported by the in situ IR data.

The corresponding spectroscopic information is summarized in Figs. 4–7. Changes in the characteristic carbonyl band are shown in Fig. 4. Increasing oxygen content red-shifted the

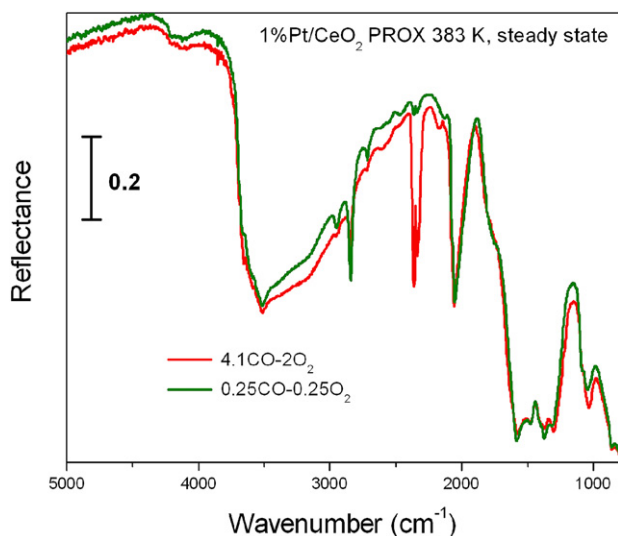


Fig. 3. DRIFT spectra of 1% Pt/CeO₂ at $T = 383$ K in two different PROX mixtures (4.1% CO/2% O₂ and 0.25% CO/0.25% O₂ in H₂).

Table 1

PROX reaction during the in situ DRIFTS experiment

	0.25% O ₂ (0.23% CO)	0.5% O ₂ (0.24% CO)	0.9% O ₂ (0.24% CO)	1.7% O ₂ (0.25% CO)
X_{CO} (%)	26.1	31.7	35.0	36.5
X_{O_2} (%)	73.0	72.9	70.2	68.3
S (%)	16.9	10.7	6.8	3.9
CO ₂ produced (mbar)	0.6	0.76	0.86	0.91
	0.25% CO (1.7% O ₂)	0.8% CO (1.7% O ₂)	1.9% CO (1.8% O ₂)	4.1% CO (2.0% O ₂)
X_{CO} (%)	36.5	50.6	49.2	43.8
X_{O_2} (%)	68.3	67.5	67.0	67.9
S (%)	3.9	17.5	38.0	65.8
CO ₂ produced (mbar)	0.91	4.05	9.2	17.9

Note. Reaction mixtures contained 0.25% CO, and 0.25–1.7% O₂ (O₂ excess $\lambda = 2$ –6.6) (upper part of the table), and 1.7–2 mbar O₂ and 0.25–4% CO (down) both series is balanced with H₂. $T = 383$ K.

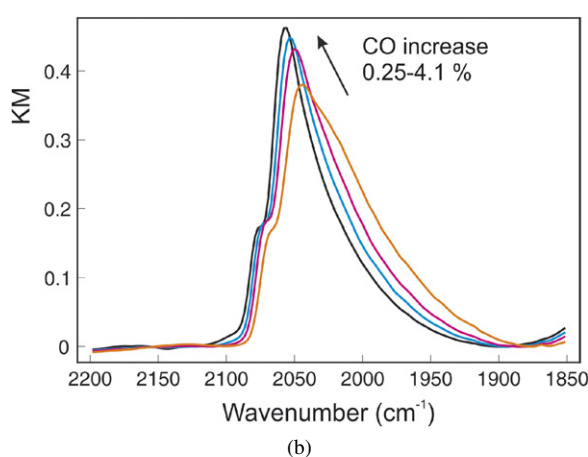
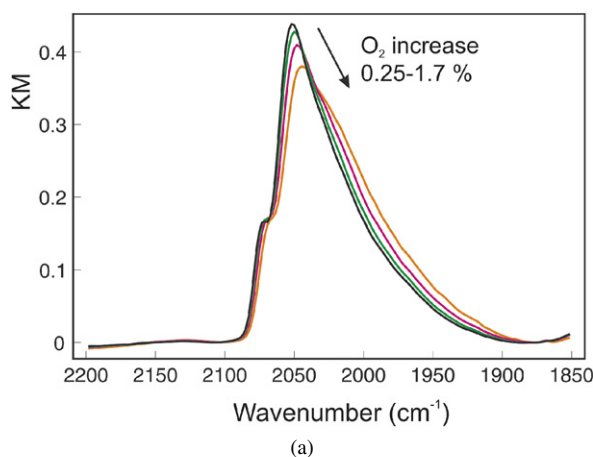


Fig. 4. DRIFT spectra in the 2200 – 1850 cm^{-1} region—CO vibrations—of 1% Pt/CeO₂ in the presence of different PROX mixtures at 383 K (a), O₂ content is varied (0.25, 0.5, 1 and 2%) at constant CO (0.25%) content; (b) CO content is varied (0.25, 0.8, 1.9 and 4.1%) at approx. constant O₂ (1.7–2%) content.

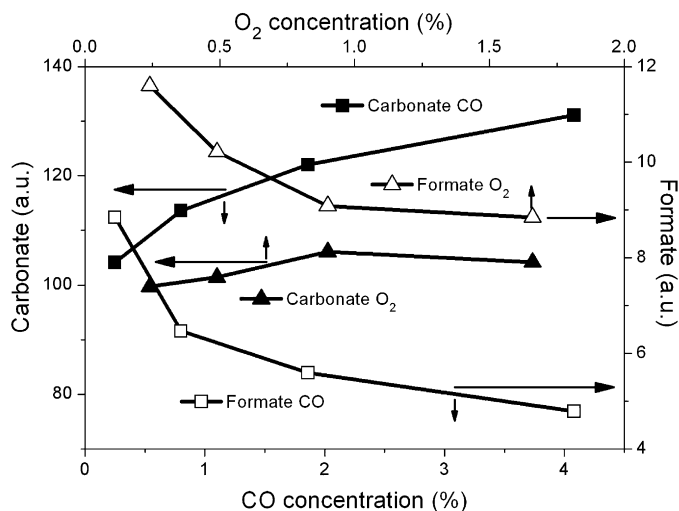


Fig. 5. Integrated intensity of formate and carbonate bands as a function of O_2 and CO content of the PROX feed. $T = 383$ K.

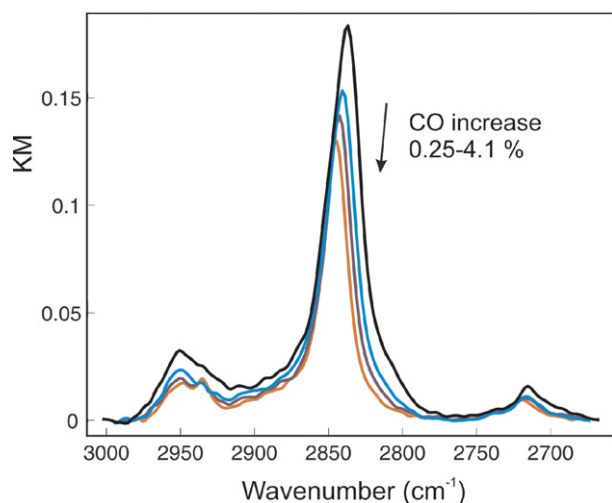


Fig. 6. DRIFT spectra in the $3000\text{--}2690\text{ cm}^{-1}$ region—CH vibrations—of 1% Pt/CeO₂ at $T = 383$ K in different PROX mixtures. CO content is varied (0.25, 0.8, 1.9 and 4.1%) at approx. constant O_2 (1.7–2%) content.

overall carbonyl band up to 7 cm^{-1} and decreased the intensity at the maximum by approximately 15%, whereas intensity developed at ~ 2020 and $\sim 1970\text{ cm}^{-1}$. Opposite changes occurred in the second experiment with increased CO concentration (Fig. 4b). The carbonyl band at the highest CO level was slightly more intense ($\sim 5\%$) and blue-shifted slightly from the original spectra in the first series, as depicted in Fig. 3. In addition, intensity at the low wavenumber side of the linear carbonyl band was lower at high CO levels. These alterations indicate that along with the insignificant changes in carbonyl coverage, Pt particles might undergo restructuring under different PROX conditions.

Alterations in the integrated intensities of formates and carbonates are depicted in Fig. 5. In both sets of experiments, these species had a complementary behavior, with carbonates typically increasing and formates decreasing. Less significant changes were found in the first experiment when more O_2 was added into the feed. The main formate band at $\sim 2840\text{ cm}^{-1}$ —

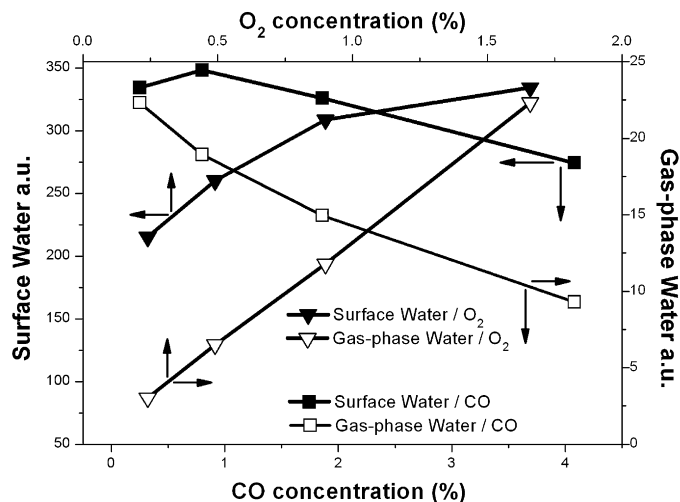


Fig. 7. Integrated intensity of surface water as a function of O_2 and CO content of the PROX feed. Concentration of gas-phase water according to the MS data in both series are also shown. $T = 383$ K.

besides decreasing—red-shifted by 4 cm^{-1} with increasing O_2 and blue-shifted by 8 cm^{-1} (Fig. 6) as a function of CO partial pressure. Although the overall carbonate intensity increased, unidentate carbonate decreased by approximately 15% in the second experiment when CO was increased. The intensity of surface water increased significantly (up to $\sim 50\%$) with increasing $p(O_2)$, whereas it went through a maximum and decreased slightly in the second set of experiments (Fig. 7).

3.3. High-pressure XPS

Similar to DRIFTS, two sets of measurements were performed in the high-pressure XPS experiments (summarized in Table 2):

- In the first set, the oxygen excess was increased (partial pressure of O_2 : 0.015–0.12 mbar) up to $\lambda = 8$.
- In the second set, the CO pressure was increased so that λ again reached 1.

Although the applied pressure was approximately only 1 mbar in these experiments, the catalytic tendencies closely resemble those seen in the flow reactor. CO conversion increased significantly but $X(O_2)$ increased only slightly in the first measurement set; selectivity decreased as a function of O_2 partial pressure and increased with increasing CO; and in the second experiment, more CO_2 was produced and $X(O_2)$ decreased slightly, as did the amount of byproduct water.

Fig. 8 depicts a part of the Ce 3d region under different experimental conditions. The catalyst pretreated in oxygen was completely oxidized to Ce^{4+} . In hydrogen, surface reduction occurred; that is, the top layers of ceria were in the Ce^{3+} state, in good agreement with TPR findings [31]. As we reported recently [18], ceria clearly reoxidized when $CO + O_2$ was introduced into the hydrogen feed; however, cerium was never purely Ce^{4+} during the PROX reaction. Broadening of the v^0 ($\sim 882.4\text{ eV}$) state toward higher binding energy was

Table 2
PROX reaction during the high-pressure XPS experiment

	0.015 mbar O ₂	0.03 mbar O ₂	0.06 mbar O ₂	0.12 mbar O ₂
X _{CO} (%)	5.4	8.5	13.2	18.6
X _{O₂} (%)	12.2	12.2	13.5	14.0
S (%)	44.3	34.9	24.3	16.6
CO ₂ produced (mbar, 10 ⁺³)	1.63	2.55	3.95	5.57
	0.03 mbar CO	0.06 mbar CO	0.12 mbar CO	0.24 mbar CO
X _{CO} (%)	18.6	15.1	12.0	7.8
X _{O₂} (%)	14.0	12.9	11.7	11.2
S (%)	16.6	29.3	51.3	69.7
CO ₂ produced (mbar, 10 ⁺³)	5.57	9.05	14.4	18.8

Note. Reaction mixtures contained 0.03 mbar CO, and 0.015–0.12 mbar O₂ (O₂ excess $\lambda = 1$ –8) (upper part of the table), and 0.12 mbar O₂ and 0.03–0.24 mbar CO (down); both series in 0.72 mbar H₂. $T = 393$ K.

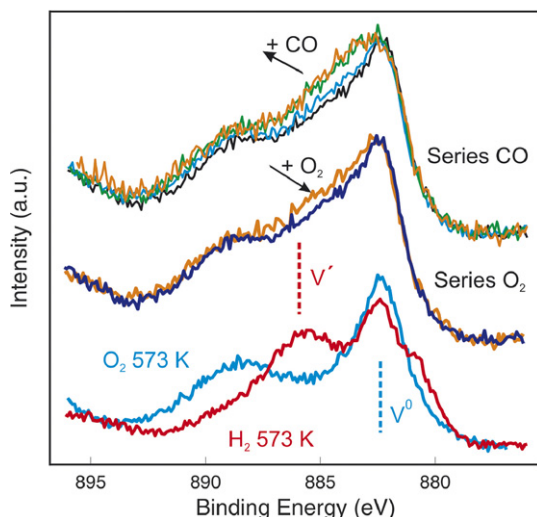


Fig. 8. Part of the Ce 3d region of the 5% Pt/CeO₂ at different conditions: (i) in 0.5 mbar O₂ at 573 K, and in 0.48 mbar H₂ at 573 K; (ii) in ~ 1 mbar PROX mixture at 393 K in the O₂ series (O₂: 0.015 and 0.12 mbar); (iii) in ~ 1 mbar PROX mixture at 393 K in the CO series (CO: 0.03–0.24 mbar).

observed, which was more pronounced with more CO in the feed. This CO-enhancing feature is situated between the v' (~ 885.8 eV; Ce³⁺) and v^0 (Ce⁴⁺) states and corresponds formally to an intermediate oxidation state. We have shown by high-resolution transmission microscopy (HRTEM) that ceria exists mainly in an oxygen-deficient CeO_{1.695} bulk structure during the PROX reaction [18,32]. The broad feature around 884.0 eV represents the surface termination of the bulk vacancy structure identified in the microscope. Excess oxygen clearly suppressed the formation of such defect sites, whereas more CO (even at the same $\lambda = 1$) enhanced the partial reduction of ceria.

Fig. 9 compares the oxygen 1s core level of 5% Pt/ceria in the second set of experiments when CO was added stepwise to the initial reaction mixture of $\lambda = 8$. The main part of the spectrum originates from the surface of the catalyst, whereas the narrow peaks on the left side correspond to the gas-phase components. Because platinum covers only $\sim 2\%$ of the surface of ceria, essentially all of the surface information should be related to the ceria. Moreover, all of the different surface species seen in IR (carbonates, formate, carbonyl, OH, ad-

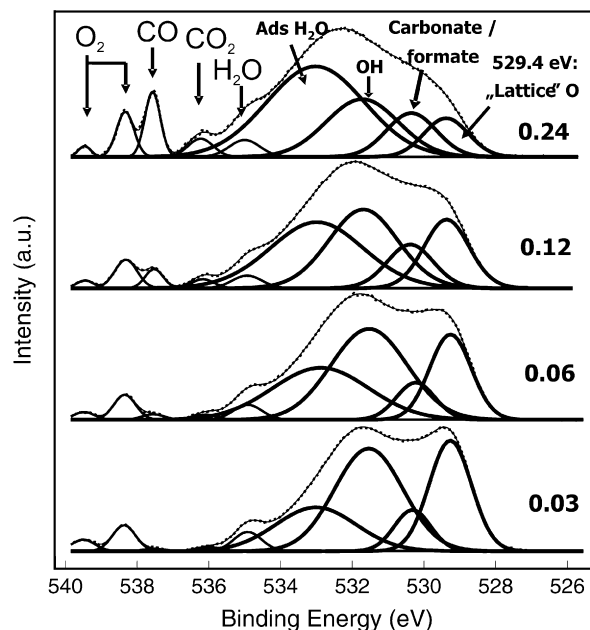


Fig. 9. O 1s spectra of the 5% Pt/CeO₂ at 393 K in the CO series of PROX mixtures (CO: 0.03–0.24 mbar). A non-constrained GL curve was used to fit adsorbed water to account for the broadening at the high BE side of the surface peak at high CO content in the feed.

sorbed water) contribute to the surface signal. Therefore, it is not surprising that deconvolution is not necessarily straightforward here. Nonetheless, following the fitting procedure that we reported recently [18], we can differentiate among ceria lattice oxygen (529.4 eV), chemisorbed oxygenates (carbonates, formates; ~ 530.5 eV), OH groups (531.5 eV; oxygenates might be obscured here as well), and adsorbed water (~ 533.0 eV). Increasing CO content in the feed reduces the fraction of lattice oxygen, in line with the partial reduction of ceria, and furthermore, the high-binding energy side of the surface spectrum increased and broadened toward higher BE, indicating more water on ceria. In the first series—increasing the O₂ partial pressure—O 1s spectra were quite independent of $p(\text{O}_2)$ (not shown separately).

The platinum 4f core levels of Pt/ceria in the second series, when changing the CO partial pressure, are shown in Fig. 10. For comparison, Pt 4f, measured in H₂ and after O₂ treatment,

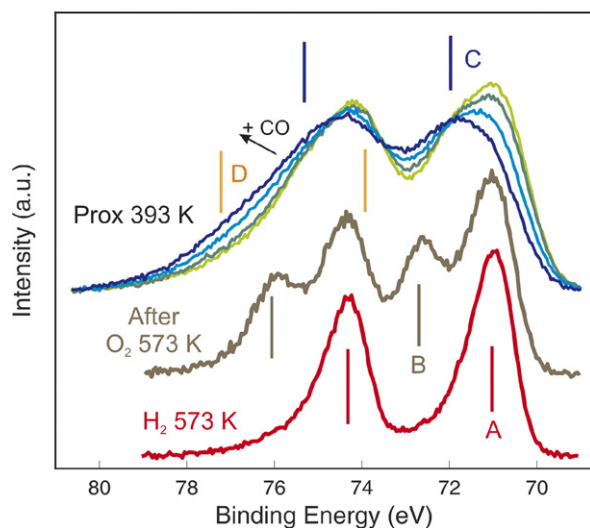


Fig. 10. Pt 4f region of 5% Pt/CeO₂ at different conditions: (i) in 0.5 mbar H₂ at 573 K; (ii) in 0.5 mbar H₂ at RT after 0.48 mbar O₂ treatment at 573 K; (iii) in ~1 mbar PROX mixtures at 393 K in the CO series (CO: 0.03–0.24 mbar). Labeled bars mark: A, metallic Pt; B, CO induced core level shift; C, interface Pt; and D, oxidized Pt.

is also included. According to the figure, platinum exists in different chemical states during the PROX reaction. Metallic Pt (71.0 eV), surface atoms linearly adsorbing CO (CO-induced surface core level shift; 72.0 eV), interface with Pt at the Pt-oxidized ceria boundary (72.6 eV), and oxidized Pt (~74.0 eV) is produced during the reaction. By adding more CO into the feed, less metallic Pt and more Pt in other states (i.e., oxidized, CO-induced, and interface) were observed.

4. Discussion

4.1. Surface species under PROX reaction

Through partial pressure-dependent in situ spectroscopic experiments, we monitored in parallel the modification of catalytic activity and the surface chemical state. We also quantified the corresponding changes in the population of surface species. The different experiments revealed very similar catalytic trends (Fig. 1; Table 1; Table 2). Consequently, despite the different actual values of conversion and selectivity (as described in detail previously [18]), the trends observed for surface species (DRIFTS) and surface oxidation states (XPS) can be considered general responses to the systematic variation of the partial pressure of a given reactant. In other words, surface species can be considered to follow the same trend during the DRIFTS and XPS measurements with, for example, changes in CO partial pressure; this holds for oxidation states as well. Further, similar to the variation in actual catalytic values in different setups, the quantities measured by spectroscopic techniques (e.g., concentration of surface species, vacancy density) cannot be transferred directly one by one from IR to XPS (or vice versa) through the 3 orders of magnitude pressure difference. Only spectroscopic trends will be similar and thus transferable.

First, Pt-carbonyl species must be taken under consideration as an obvious candidate for a reaction intermediate in CO

oxidation. The coverage with linear carbonyls decreased only slightly when the oxygen content of the feed was increased (Fig. 4a), as did the reaction rate. This finding is in good accordance with the traditional mechanism of CO oxidation on platinum [33,34], in as much as O₂ activation and oxidation are possible only when carbonyl coverage is incomplete. In contrast, adding increasing amounts of CO to the O₂-rich feed increased the amount of linear carbonyls (Fig. 4b) and drastically improved the activity (Table 1). Obviously, in the case of reducible supports (especially on ceria), oxygen can be activated on the support site, and can react with CO through spillover to the Pt particles or at the metal-support interface; thus no activation of O₂ on Pt is necessary [17,35]. But can the small increase in carbonyls explain the 20-fold increase in CO₂ production with increasing CO concentration in the DRIFTS cell from 0.25 to 4% (cf. Table 1 and Fig. 4b)? Moreover, the carbonyl bands at 0.25% CO/0.5% O₂ and 0.8% CO/1.7% O₂ are identical (compare them in Figs. 4a and 4b) even with a more than fivefold difference in CO oxidation activity. Therefore, we can conclude that although linear carbonyls may play an important role (as an intermediate) on Pt/ceria in the PROX reaction, their surface coverage certainly does not determine the CO oxidation activity. Furthermore, the changes seen in the Pt-carbonyl band (Fig. 4) and Pt 4f spectra probably are not two independent processes, and morphological alteration of Pt nanoparticles may be partly responsible for both variations. Such restructuring could be induced by the red-ox changes of ceria at different feed compositions (similar to the observation on Cu/ZnO [36,37]), giving rise to surface wetting at more reduced ceria. Note that changes in Pt-carbonyl are likely due to both slight coverage and morphological modification [38,39].

Formate species correlated negatively with CO oxidation activity in both experiments (see Fig. 5, Table 1). There are four explanations for such a correlation. First, formates could act as reaction intermediates in the CO oxidation route, and their decomposition is rate-determining. Second, formates could block catalytic sites or at least hinder a surface process relevant to achieve good activity. Third, the presence of formates can be an indicator of a surface state that is not beneficial for CO oxidation in the presence of hydrogen. Fourth, it could have occurred accidentally (i.e., the increased activity and decreased formate band intensity are two independent processes).

The first model was applied to explain CO₂ production in the WGS reaction [16,40]. In the WGS reaction, formate decomposition by their interaction with water (to produce unidentate carbonate and H₂) was suggested to be the rate-limiting step. We consider this route or a similar mechanism involving formates not likely here, however. First, those studies [16,31] were carried out at a temperature about 100–150 K higher than in this study ($T = 383$ K in our case). Second, the intensity of formates (according to the peak integral) decreased from ~11.6 to ~8.8 (factor of 1.3) when the oxygen concentration was changed, whereas CO oxidation increased by a factor of ~1.5. In the second set of experiments, formates dropped from ~8.8 to ~4.8 (by a factor of 1.8), whereas the amount of produced CO₂ increased 20 times. The proportionality between the changes in formate intensity and activity differed signifi-

cantly in the two cases; therefore, the changes in the formate concentration alone cannot explain the changes in the activity (expressed as CO molecules converted to CO₂ molecules). For this same reason, the second possibility (i.e., a site-blocking effect), although possible, by itself is not sufficient to explain the activity changes.

Concerning the last two possible explanations, the amount of formates was highest when both CO and O₂ concentrations were the lowest. Furthermore, the situation of the lowest CO and O₂ concentrations represents the highest H_{ads} concentration on the platinum particles among the conditions studied and likely the highest spillover rate of H toward the ceria as well. Hydrogen partially reducing the surface of ceria creates OH groups (especially type IIB [41,42]), which react with CO to form formates [43]. Therefore, the highest formate population is likely to imply the highest hydrogen spillover rate from platinum toward the ceria. Moreover, as formates decreased, carbonates (except unidentate) always increased (Fig. 5), indicating the transformation of formates to carbonates. However, H₂ alone—when reducing the catalyst at 573 K—produced only a small formate band (not shown) by partial reduction of carbonates initially present on the surface. Thus the presence of gas-phase CO (or CO₂) is essential to form formates. In a previous study [18], we compared the evolution of surface species in the presence of CO alone, CO + O₂ in He, and the PROX mixture (CO + O₂ in H₂). The formation of formate species was suppressed by the presence of oxygen (CO + O₂) and was most pronounced in the presence of the PROX mixture.

Based on the aforementioned considerations, we propose that an equilibrium exists between formate and carbonate species and that their actual abundance is a strong function of surface hydrogen and oxygen concentration, of the availability of OH groups, and thus of gas-phase composition. This equilibrium can be related to the amount of produced CO₂ but by itself cannot explain the changes in CO oxidation activity in the PROX reaction.

Concerning the undesired side reaction, water can be produced when O_{ads} and H_{ads} are adjacent; however Ertl [44] has shown that reaction (A) is much faster than reaction (B):



Because O₂ rapidly reoxidizes reduced-ceria surface even at room temperature (as we previously demonstrated by high-pressure XPS [18]), we can assume that O_{ads} will be available on ceria if O₂ is present in the gas phase. Water production on Pt (especially when introducing a PROX mixture to the pre-oxidized catalyst) cannot be completely neglected, but more likely, H_{ads} spills over onto the ceria and reacts with the first OH group forming surface water. In this way, production of surface water is a function of H spillover rate and O₂ concentration in the gas phase. In steady-state operation, surface water is in equilibrium with gas-phase water; thus, the latter also should be a function of H spillover rate and gas-phase O₂ concentration.

4.2. Structural changes/oxygen vacancies

In situ XPS indicated that the surface of ceria contains oxygen vacancies (i.e., is partly reduced), and that the concentration of those vacancies decreased with addition of O₂ and increased with increasing CO in the gas feed (Fig. 8). It was shown that a perfect, nonreduced ceria is not effective in adsorbing significant amounts of water and thus building up an intermolecular H-bonding network [45]. Therefore, the surface/gas-phase equilibrium of water (i.e., desorption of surface water) is expected to be a significant function of surface defects and thus a function of feed composition. Indeed, an approximately 50% increase in surface water concentration as a function of $p(\text{O}_2)$ (Fig. 7) can be understood as the convolution of a strong increase in water production (open triangles in Fig. 7) and a decrease in vacancy concentration (similar to that shown Fig. 8). (Note again that the trends are transferable only between XPS and DRIFTS.) The maximum type (decreasing) curve with increasing $p(\text{CO})$ is the result of decreased gas-phase water production (open squares in Fig. 7) and increasing vacancy density. During XPS, the strong effect of vacancy formation (Fig. 8) seems to overcompensate for the loss of water production, resulting in an increasing surface water concentration. Therefore, vacancy formation seems to be slightly more pronounced in the reaction feeds applied during XPS than at atmospheric conditions.

In an earlier communication [18], we suggested that the preferential CO oxidation on Pt/ceria is related to the presence of adsorbed water, and that CO₂ is produced at the phase boundary between Pt and ceria by the interaction of carbonyl and activated water. Considering the foregoing discussion on the abundance of different surface species, we can conclude that their coverage by itself is not able to control the PROX activity. PROX performance improved significantly at higher $p(\text{CO})$, which increased the number of oxygen vacancies on the ceria surface. Water stabilized on such a vacancy ceria site slows further water production by poisoning H oxidation sites by hindering desorption, and thus improves selectivity. This is in complete agreement with the perfect positive correlation of decaying surface water concentration and decreasing CO₂ production as a function of temperature [46], because H₂O_{ads} desorption liberates active sites for H₂ oxidation at full oxygen conversion, shifting the selectivity toward hydrogen oxidation.

A possible explanation for the enhanced activity with hydrated vacancy-rich ceria could be that the catalyst itself adapts to the reaction feed composition. The transition state of the rate-determining step can be reached more easily in this way, and thus the activation energy (E_a) of the reaction decreases when the surface properties of the catalyst change, that is, with changing feed composition (CO and O₂ partial pressures). To validate this hypothesis, the temperature dependence of the CO oxidation rate was measured for calculating apparent activation energies (app. E_a) at two different feed compositions (4% CO, 2% O₂ and 0.25% CO, 0.25% O₂, both in H₂). These data are compared in Fig. 11. The apparent activation energy was approximately 18 kJ/mol lower with the higher CO + O₂ content feed (4% CO, 2% O₂). This lower appar-

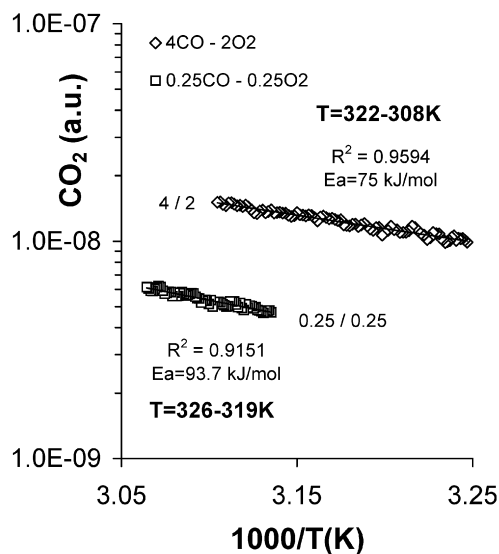


Fig. 11. Arrhenius plot for 1% Pt/CeO₂ in PROX reaction at two different feed compositions (4% CO + 2% O₂ in H₂ and 0.25% CO and 0.25% O₂ in H₂). Temperature range: 308–326 K.

ent activation energy may be due to (i) lower activation energy of the rate-determining step, (ii) changes in the reaction order, or (iii) higher adsorption enthalpy at the higher concentration. We recently demonstrated that the coverage with surface Pt-carbonyls on Pt/ceria was independent of reaction temperature below 420 K under PROX conditions [46]; thus, so it is not likely that the adsorption enthalpy changes and plays a significant role here. Furthermore, based on the discussion of the DRIFTS results, we might assume that changes in apparent activation energy should originate mainly from the activation energy of the rate-determining step rather than from alterations in the reaction order. The lower apparent activation energy at higher CO + O₂ content could account for a dramatic increase in the CO oxidation rate, to levels even significantly higher than observed here.

Because correlation between surface species and activity alone cannot fully explain the activity changes, we suggest that the modification of the surface state is the driving force behind the lower activation energy, higher CO oxidation activity, and accordingly higher selectivity toward CO oxidation. This modification involves the creation of a significant amount of reduced ceria sites (increase in O-vacancies), greatly decreasing the possibility of water desorption. This model is in good accordance with the finding of decreased CO oxidation selectivity with increasing temperature ([18,46]; also see Fig. 2) as well as with the fact that the best PROX performance (98–99% CO conversion) on Pt/ceria was achieved at fairly low temperature (333–343 K). Moreover, reversible Pt structural modification is also likely involved in the catalyst transformation, giving rise to altered performance with changing feed composition. Further studies could clarify this point.

The results presented here reinforce the view that the surface of a catalyst is meta-stable with respect to its as-synthesized form. Its interaction with the reactant gases turns the synthesized “precursor” state to a “real” catalyst. The changes in the

evolution of (IR-detectable) surface species can be understood as either a cause or consequence of these structural responses; distinguishing between these two possibilities may be impossible in some cases.

5. Conclusion

Multiple steady-state in situ spectroscopic (DRIFTS and XPS) experiments were carried out to correlate activity changes, surface species, and chemical states in the preferential oxidation of CO in the presence of hydrogen (PROX reaction). The “classical” mechanism of low-temperature CO oxidation on ceria-supported Pt [16,35], a noncompetitive mechanism (i.e., CO adsorption on metal and oxygen activation on the support), and reaction on the metal/oxide interface may be possible here as well. The changes seen in the Pt-carbonyl band, however, indicate that this type of reaction is not determined by the availability of CO species on Pt particles, because of the insignificant correlation between Pt–CO and CO₂ production. Formate species showed clear negative correlation with CO oxidation activity. The proportionality between the amount of formates and CO₂ production differed greatly in the two cases when oxygen and CO concentration were increased stepwise. We propose that these are not reaction intermediates. Their evolution can be interpreted as resulting from a distorted equilibrium transformation between surface carbonates and formates induced by changes in gas-phase composition, surface H_{ads} concentration (i.e., availability of type IIB OH groups), and surface structure.

Oxygen vacancy formation detected by in situ high-pressure XPS showed good correlation with enhanced CO oxidation activity. Water desorption was hindered at higher vacancy densities, however. Highly hydrated ceria with significant vacancy density is believed to be beneficial for the PROX process. Here surface water blocks H_{ads} oxidation sites, making more oxygen available for the desired CO oxidation reaction. Moreover, lower apparent activation energy of CO oxidation was measured in the PROX reaction on catalysts with greater numbers of vacancies. The evolution of surface species also can be interpreted as a consequence of the changes in surface chemical state.

From a general standpoint, we suggest that the surface of an effective catalyst can adapt to the reaction conditions in a way that is beneficial for the reactions, with decreased activation energy, a decreased number of “blocking species,” and increased mobility of surface species active in the desired reaction or sometimes decreased mobility and desorption of undesired side products.

Acknowledgments

This work was supported by the Hungarian National Science Foundation (grant OTKA F046216), Hungarian National R&D Program (grant NKFP 3A058-04), and the Athena Consortium. A.W. thanks the Bolyai Grant of the Hungarian Academy of Sciences. The authors thank the BESSY staff for their technical assistance with the in situ XPS measurements.

References

- [1] R.A. van Santen, M. Neurock, *Catal. Rev. Sci. Eng.* 37 (4) (1995) 557.
- [2] M. Neurock, *J. Catal.* 216 (2003) 73.
- [3] K. Reuter, D. Frenkel, M. Scheffler, *Phys. Rev. Lett.* 93 (2004) 116105.
- [4] B. Hammer, O.H. Nielsen, J.K. Nørskov, *Catal. Lett.* 46 (1997) 31.
- [5] B.M. Weckhuysen (Ed.), *In Situ Spectroscopy of Catalysts*, ASP, North Lewis Way, 2005.
- [6] G.J. Hutchings, A. Desmartin-Chomel, R. Olier, J.C. Volta, *Nature* 368 (1994) 41.
- [7] J.M. Thomas, *Angew. Chem. Int. Ed.* 38 (1999) 3589.
- [8] H. Topsøe, *J. Catal.* 216 (2003) 155.
- [9] J.D. Grunwaldt, A. Baiker, *Phys. Chem. Chem. Phys.* 7 (2005) 3526.
- [10] M. Hunger, J. Weitkamp, *Angew. Chem. Int. Ed.* 40 (2001) 2954.
- [11] A.J. Appleby, F.R. Foulkes, *Fuel Cell Handbook*, Van Nostrand Reinhold, New York, 1989.
- [12] R.A. Lemons, *J. Power Sources* 29 (1990) 251.
- [13] J.N. Armor, *Appl. Catal.* 176 (1999) 159.
- [14] T. Bunluesin, R.J. Gorte, G.W. Graham, *Appl. Catal. B* 15 (1998) 107.
- [15] Q. Fu, A. Weber, M. Flytzani-Stephanopoulos, *Catal. Lett.* 77 (2001) 87.
- [16] G. Jacobs, L. Williams, U. Graham, D.E. Sparks, B.H. Davis, *J. Phys. Chem. B* 107 (2003) 10398.
- [17] A. Wootsch, C. Descorme, D. Duprez, *J. Catal.* 225 (2004) 259.
- [18] O. Pozdnyakova, D. Teschner, A. Wootsch, J. Kröhnert, B. Steinhauer, H. Sauer, L. Toth, F.C. Jentoft, A. Knop-Gericke, Z. Paál, R. Schlögl, *J. Catal.* 237 (2006) 1.
- [19] O. Pozdnyakova, D. Teschner, A. Wootsch, J. Kröhnert, B. Steinhauer, H. Sauer, L. Toth, F.C. Jentoft, A. Knop-Gericke, Z. Paál, R. Schlögl, *J. Catal.* 237 (2006) 17.
- [20] S. Kacimi, J. Barbier Jr., R. Taha, D. Duprez, *Catal. Lett.* 22 (1993) 343.
- [21] As higher metal loading and lower pressure did not critically influence the catalytic function during XPS measurements, the tendencies in the chemical state of the catalyst observed as a function of O₂ or CO partial pressure can be regarded as typical during PROX reaction on Pt/ceria.
- [22] D.F. Ogletree, H. Bluhm, G. Lebedev, C. Fadley, Z. Hussain, M. Salmeron, *Rev. Sci. Instrum.* 73 (2002) 3872.
- [23] P. Burroughs, A. Hamnett, A.F. Orchard, G. Thornton, *J. Chem. Soc. Dalton Trans.* 17 (1976) 1686.
- [24] M.J. Kahlich, H.A. Gasteiger, R.J. Behm, *J. Catal.* 171 (1997) 93.
- [25] M.J. Kahlich, H. Gasteiger, R.J. Behm, *J. Catal.* 182 (1999) 430.
- [26] B. Schumacher, Y. Denkwitz, V. Plzak, M. Kinne, R.J. Behm, *J. Catal.* 224 (2004) 449.
- [27] C. Binet, M. Daturi, J.-C. Lavalley, *Catal. Today* 50 (1999) 207.
- [28] C. Li, T. Arai, K. Domen, K. Maruya, T. Onishi, *J. Chem. Soc. Faraday Trans.* 85 (1989) 929.
- [29] C. Li, Y. Sakata, T. Arai, K. Domen, K. Maruya, T. Onishi, *J. Chem. Soc. Faraday Trans.* 85 (1989) 1451.
- [30] T. Shido, Y. Iwasawa, *J. Catal.* 136 (1992) 493.
- [31] G. Jacobs, A. Robert, K. Burtron, B.H. Davis, *J. Catal.* 245 (2007) 326.
- [32] D. Teschner, A. Wootsch, O. Pozdnyakova, H. Sauer, A. Knop-Gericke, R. Schlögl, *React. Kinet. Catal. Lett.* 87 (2006) 235.
- [33] C.T. Campbell, G. Ertl, H. Kuipers, J. Segner, *J. Chem. Phys.* 73 (1980) 5862.
- [34] M.A. Barteau, E.I. Ko, R.J. Madix, *Surf. Sci.* 104 (1981) 161.
- [35] Y.Y. Yung-Fang, *J. Catal.* 87 (1984) 162.
- [36] P.L. Hansen, J.B. Wagner, S. Helveg, J.R. Rostrup-Nielsen, B.S. Clausen, H. Topsøe, *Science* 295 (2002) 2053.
- [37] J.D. Grunwaldt, A.M. Molenbroek, N.Y. Topsøe, H. Topsøe, B.S. Clausen, *J. Catal.* 194 (2000) 452.
- [38] D.W. Daniel, *J. Phys. Chem.* 92 (1988) 3891.
- [39] T. Jin, Y. Zhou, G.J. Mains, J.M. White, *J. Phys. Chem.* 91 (1987) 5931.
- [40] T. Shido, Y. Iwasawa, *J. Catal.* 141 (1993) 71.
- [41] A. Tsyganenko, V. Filimonov, *J. Mol. Struct.* 19 (1973) 579.
- [42] A. Badri, C. Binet, J.C. Lavalley, *J. Chem. Soc. Faraday Trans.* 92 (1996) 4669.
- [43] G. Jacobs, U.M. Graham, E. Chenu, P.M. Patterson, A. Dozier, B.H. Davis, *J. Catal.* 229 (2005) 499.
- [44] G. Ertl, *Chem. Rec.* 1 (2001) 33.
- [45] M.A. Hendreson, C.L. Perkins, M.H. Engelhard, S. Thevuthasan, C.H.F. Peden, *Surf. Sci.* 526 (2003) 1.
- [46] O. Pozdnyakova-Tellinger, D. Teschner, J. Kröhnert, F.C. Jentoft, A. Knop-Gericke, R. Schlögl, A. Wootsch, *J. Phys. Chem. C* 111 (2007) 5426.